AMERICAN SOCIETY FOR MICROBIOLOGY | mBio

Check for updates

| Pathogenesis and Host Response | Research Article

Diet composition drives tissue-specific intensity of murine enteric infections

Helene Israelson,[1] Amalie Vedsted-Jakobsen,[1] Ling Zhu,[1] Aurelie Gagnaire,[2] Alexandra von Münchow,[1] Nina Polakovicova,[1] Angela H. Valente,[1] Ali Raza,[1] Audrey I. S. Andersen-Civil,[1] John E. Olsen,[1] Laura J. Myhill,[1] Peter Geldhof,[2] Andrew R. Williams[1]

AUTHOR AFFILIATIONS See affiliation list on p. 19.

ABSTRACT Diet composition plays a large role in regulating gut health and enteric infection. In particular, synthetic "Western-style" diets may predispose to disease, while whole-grain diets containing high levels of crude fiber are thought to promote gut health. Here, we show that, in contrast to this paradigm, mice fed with unrefined chow are significantly more susceptible to infection with *Trichuris muris*, a caecum-dwelling nematode, than mice fed with refined, semi-synthetic diets (SSDs). Moreover, mice fed with SSD supplemented with inulin, a fermentable fiber, developed chronic *T. muris* burdens, whereas mice fed with SSD efficiently cleared the infection. Diet composition significantly impacted infection-induced changes in the host gut microbiome. Mice infected with the bacterium *Citrobacter rodentium* were also more susceptible to pathogen colonization when fed with either chow or inulin-enriched SSD. However, transcriptomic analysis of tissues from mice fed with either SSD or inulin-enriched SSD revealed that, in contrast to *T. muris*, increased *C. rodentium* infection appeared to be independent of the host immune response. Accordingly, exogenous treatment with interleukin (IL)-25 reduced *T. muris* burdens in inulin-fed mice, whereas IL-22 treatment was unable to restore resistance to *C. rodentium* colonization. Diet-mediated effects on pathogen burden were more pronounced for large intestine-dwelling pathogens, as effects on small the intestinal helminth (*Heligmosomoides polygyrus*) were less evident, and protozoan (*Giardia muris*) infection burdens were equivalent in mice fed with chow, inulin-enriched SSD, or SSD, despite higher cyst excretion in chow-fed mice. Collectively, our results point to a tissue- and pathogen-restricted effect of dietary fiber levels on enteric infection intensity.

IMPORTANCE Enteric infections induce dysbiosis and inflammation and are a major public health burden. As the gut environment is strongly shaped by diet, the role of different dietary components in promoting resistance to infection is of interest. While diets rich in fiber or whole grain are normally associated with improved gut health, we show here that these components predispose the host to higher levels of pathogen infection. Thus, our results have significance for interpreting how different dietary interventions may impact on gastrointestinal infections. Moreover, our results may shed light on our understanding of how gut flora and mucosal immune function is influenced by the food that we eat.

KEYWORDS diet, helminths, *Giardia*, *Citrobacter*, immune response

Enteric parasitic and bacterial infections are among the top 10 causes of death worldwide. More than 1.5 billion people are infected globally with parasitic worms (helminths), with millions more afflicted with bacterial infections such as *Escherichia coli*, *Clostridium difficile*, and *Salmonella* (1–3). These pathogens are also ubiquitous in livestock production systems worldwide, threatening food security and economic

Invited Editor Maria Joanna Doligalska, Uniwersytet Warszawski, Warsaw, Poland

Editor Avery August, Cornell University, Ithaca, New York, USA

Address correspondence to Andrew R. Williams, arw@sund.ku.dk.

The authors declare no conflict of interest.

See the funding table on p. 19.

Received 25 September 2023
Accepted 27 November 2023
Published 5 January 2024

development (4, 5). Antibiotic and anti-parasitic drug resistance limit effective treatment options for many of these pathogens, and thus, novel solutions are urgently required (5, 6).

There is increasing evidence that diet composition plays a key role in mediating resistance to enteric infection and inflammation. Worldwide, there is an increasing shift toward the consumption of refined diets, semi-synthetic diets (SSDs), or "Western diets" that lack crude plant fibers and phytochemicals (7). This may have profound consequences for the composition of the gut microbiota and for the activity of immune cells that reside at the mucosal barrier (8, 9). High rates of obesity and chronic diseases such as colitis may be attributed, in part, to the consumption of refined diets and associated dysbiosis and dysregulated immune function (10, 11).

Nutritional interventions may be a sustainable tool to promote resistance to enteric pathogens through modulation of mucosal immunity. Mucosal immune responses can be broadly classified as type 1, type 2, and type 3: type-1 responses protect against viruses and intracellular bacteria, while type-2 responses defend the host against parasitic worms (helminths), and type-3 responses are crucial against extracellular bacteria and fungi (12, 13). These different arms of the immune response are inter-regulated, and therefore, the relative balance of these opposing immune subsets can determine the outcome of infection. The activity of immune cells (e.g., T cells) in the gut is also continually calibrated by exposure to extrinsic factors such as diet and diet-derived metabolites (14). Dietary components may impact mucosal immune function through several overlapping mechanisms. First, the breakdown of dietary carbohydrates and proteins may favor the growth of defined gut bacteria that subsequently impact immune cell behavior (15). Second, altered gut microbiome (GM) composition resulting from changing dietary patterns can modulate the abundance of certain gut metabolites such as secondary bile acids, which can impact on immune cell function, for example, by inducing T-regulatory cells (16). Third, many dietary compounds, for example, polyphenols or carbohydrate polymers, can directly interact with intestinal epithelial cells or innate immune cells such as dendritic cells to shape the immune and inflammatory tone in the gut (17–19).

Levels of dietary macro- and micro-nutrients such as protein and zinc are known to markedly impact on the expression of immunity to enteric infections (20, 21). In addition, a number of studies in both pre-clinical models and human intervention studies have shown proof of concept that the GM and immune function can be substantially modulated by the consumption of defined dietary components such as soluble fibers, with potential benefits for metabolic disease and chronic inflammation (22–25). These and other studies have generally defined a paradigm; diets rich in crude fiber and unrefined plant material (e.g., rodent chow) promote a healthy gut and robust and balanced immune function, while purified SSD lacking in fiber can lead to dysbiosis, inflammation, and disease, especially when combined with a high level of fat and/or sucrose. However, the interactions between dietary intake and resistance to enteric infection are not yet clear. The composition of dietary fiber has been shown to have a significant influence on the severity of different infections in mice but, sometimes, with conflicting results. For example, SSD has been shown to result in more severe infections with the Gram-negative bacterium *Citrobacter rodentium* in mice compared with chow, but in other models, infections with *Salmonella* or *Listeria* are enhanced in mice fed with chow, relative to mice fed with SSD (26, 27). Further studies are clearly required to understand, in greater detail, the relationships between diet composition, mucosal immunity, and enteric infection.

Here, we show that infections in the large intestine (LI) with either the helminth parasite *Trichuris muris* or the bacterium *C. rodentium* are substantially lower when mice are fed with SSD, compared to either chow or SSD enriched with the soluble fiber inulin. We further demonstrate that while increased susceptibility to *T. muris* is associated with altered immune function and can be partially restored with exogenous administration of a type-2 polarizing cytokine, susceptibility to *C. rodentium* occurs despite an intact

immune response. Finally, we show that colonization of pathogens residing in the small intestine (SI), rather than in the caecum or colon, is less sensitive to regulation by dietary composition. Taken together, our results shed further light on diet-mediated regulation of responses to mucosal pathogens in the large and small intestinal tissues.

RESULTS

Feeding chow increases enteric pathogen burdens relative to SSDs

During a long-term project to explore the relationship between diet composition and immunity to helminths, we observed a trend in our laboratory for *T. muris* burdens to be noticeably lower in mice fed with experimental open-source SSD, compared to standard rodent chow. To examine this in detail, we utilized a chronic *T. muris* infection model in C57BL/6 mice where animals were infected with a low dose (20 eggs) repeated over several weeks and fed with either chow or SSD. Mice were fed with SSD or chow for 2 weeks prior to the commencement of infection and sacrificed 35 days post-infection (p.i.) after the first egg dose (i.e., 7 weeks of total of dietary treatment). This revealed that worm burdens were more than fourfold higher in chow-fed mice, with a substantial number of SSD-fed mice being worm-free (Fig. 1A). Analysis of earlier time points showed that at Day 11 p.i., all mice fed with SSD harbored worms (albeit significantly less so than chow-fed mice), but by Day 21 p.i., only very few worms were found in SSD-fed mice, indicating an accelerated expulsion process, rather than reduced establishment (Fig. S1). Furthermore, infected mice fed with SSD had significantly lower *T. muris*-specific IgG2a and significantly higher IgG1 antibodies in serum, indicative of a shift from a T-helper type-1 (Th1) to a T-helper type-2 (Th2) response (Fig. 1B). Regardless of diet, *T. muris* infection significantly increased the expression of *Ifng* and *Il13* in caecal tissue, but the increase in *Ifng* expression was significantly more pronounced (~1,000-fold) in the chow-fed mice than SSD-fed mice (Fig. 1C). Interestingly, the increase in *Il13* expression was also relatively higher in chow-fed mice than SSD-fed mice, however, not to the same extent as *Ifng*, indicating that the transcriptional response in chow-fed mice was polarized toward a type-1 response (Fig. 1C). As chronic *T. muris* infection induces crypt hyperplasia (28), we examined the colon for crypt lengths and goblet cell numbers. Infection significantly increased crypt length in mice fed with both diets (Fig. 1D). In accordance with the low worm numbers, crypt lengths were significantly shorter in SSD-fed mice during *T. muris* infection and also in uninfected SSD-fed mice, indicating that diet composition had a regulatory effect on the gut mucosal tissue independent of infection ($P < 0.05$ for main effects of diet and infection; Fig. 1D). Consistent with this, goblet cells were lower in uninfected mice fed with SSD compared to chow but not in *T. muris*-infected mice ($P < 0.05$ for interaction between infection and diet). Thus, *T. muris* trickle infection did not increase goblet cell numbers in chow-fed mice, consistent with previous reports (28), but did do so in SSD-fed mice. Furthermore, goblet cell size was also lower in uninfected mice fed with SSD but was boosted by *T. muris* infection, indicating that infection induced an active goblet cell hyperplasia only in mice fed with SSD (Fig. 1D). We noted a similar trend with T-cell populations in mesenteric lymph nodes (MLNs). In chow-fed mice, *T. muris* infection did not change the proportion of Th1 (Tbet$^+$) cells or Th2 (GATA3$^+$) cells (Fig. 1E and F). In SSD-fed mice, proportions of Th1 cells were significantly lower compared to chow-fed mice in the absence of infection but were increased in *T. muris*-infected mice ($P < 0.05$ for interaction between diet and infection; Fig. 1E). Th2 cells were not affected by diet in uninfected mice but were significantly higher in *T. muris*-infected mice fed with SSD, relative to infected mice fed with chow ($P < 0.05$ for interaction between diet and infection; Fig. 1F), consistent with a type-2 immune bias occurring in SSD-fed mice during *T. muris* infection. Furthermore, we observed that feeding SSD significantly decreased T-regulatory (Treg) (Foxp3$^+$) populations independently of *T. muris* infection ($P < 0.05$ for main effect of diet; Fig. 1F). Notably, these effects of diet on T-cell populations appeared to result from prolonged consumption of the diets, as at the time point that trickle infection was commenced (i.e., after 14 days of diet adaptation), no differences were observed in T-cell subsets (Fig. S2). Collectively, these

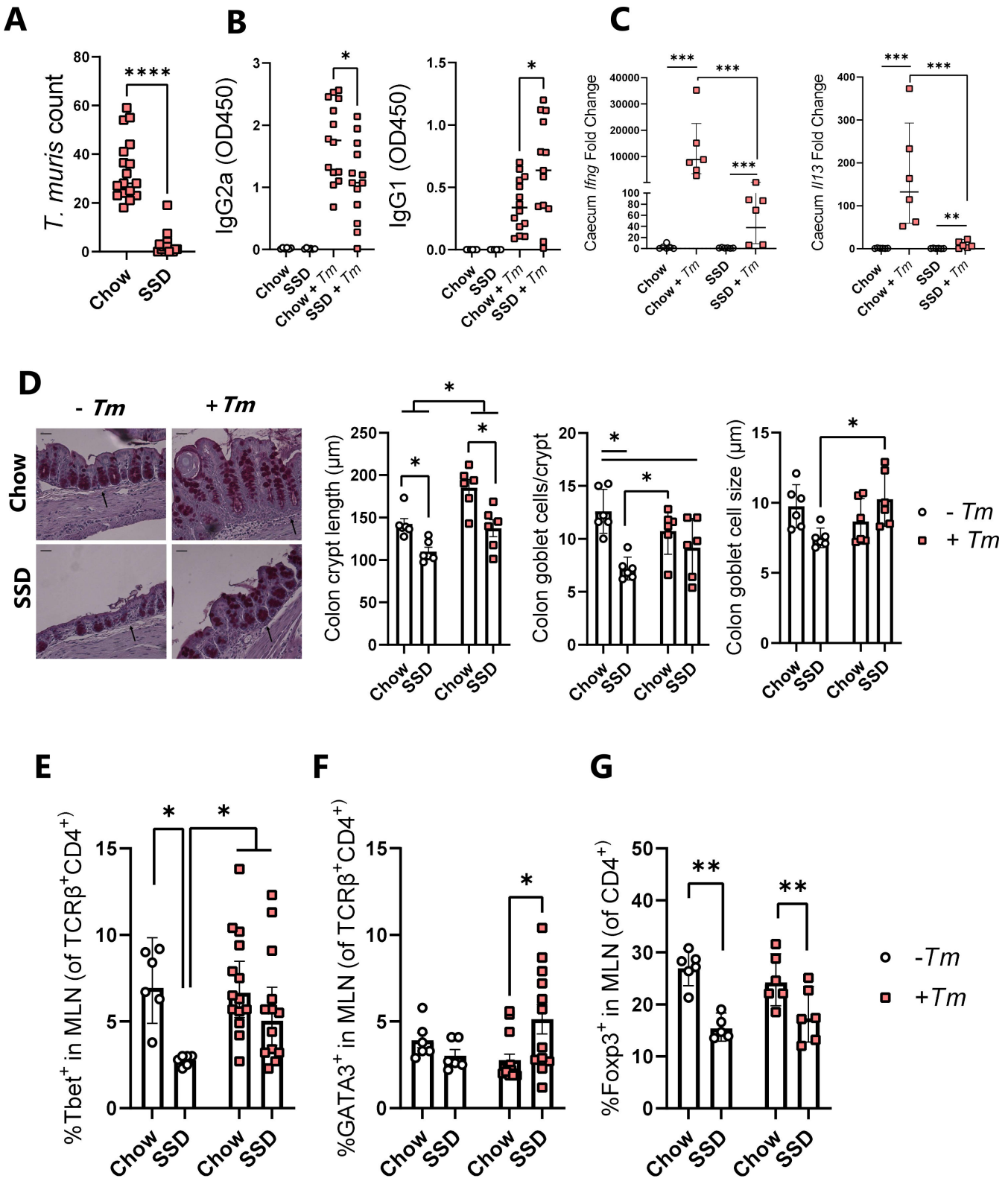

FIG 1 Impact of chow or SSDs on *T. muris* infection burdens and host immune response. Mice were fed with either chow or SSDs, trickle-infected with *T. muris* by inoculation with 20 eggs on Days 0, 7, and 14, and sacrificed on Day 35 p.i. (A) Worm burdens in caecum on Day 35 p.i. Data are from three independent experiments, each with n = 3–8 mice/dietary group. (B) *T. muris*-specific IgG2a and IgG1 levels in serum on Day 35 p.i. Data from infected mice are from two independent experiments, each with n = 6–8 mice/treatment group, and data from uninfected mice are from a single experiment with n = 6 mice/group. (C)

(Continued on next page)

FIG 1 (Continued)

Expression of *Ifng* and *Il13* assessed by qPCR in the caecum on Day 35 p.i. Data are from a single experiment, with $n = 6$ mice/treatment group. Fold changes are relative to uninfected controls within each diet group. (D) Crypt hyperplasia, goblet cell numbers, and goblet cell diameter in proximal colon samples at Day 35 p.i. Data are from a single experiment, with $n = 6$ mice/treatment group. Scale bar = 50 µm, and arrow indicates muscularis mucosae. ×200 magnification. (E and F) Percentage of Tbet$^+$ and GATA3$^+$ CD4$^+$ T cells and (G) Foxp3$^+$ CD4$^+$ cells in the MLNs of mice on Day 35 p.i. For Tbet$^+$ and GATA3$^+$ expression, data from infected mice are from two independent experiments, each with $n = 5$–8 mice/treatment group, and data from uninfected mice are from a single experiment with $n = 6$ mice/group. For Foxp3$^+$ expression, data are from a single experiment, with $n = 5$–6 mice/treatment group. See Fig. S4 for the T-cell gating strategy. $^{****}P < 0.001$, and $^{*}P < 0.05$ by Mann-Whitney test, comparing infected groups on chow and SSD (A and B). $^{***}P < 0.005$, $^{**}P < 0.01$, and $P < 0.05$ by two-way ANOVA, with Tukey's post hoc testing where interaction term is significant (C–G). Data are presented as medians (A and B), geometric means with 95% confidence intervals (C and E), or mean ± S.E.M. (D, F, and G).

data show that diet composition substantially impacted *T. muris* infection levels and that indicators of an activated type-2 immune response were more evident in SSD-fed mice than in chow-fed mice.

Due to our observation that the increased *T. muris* burdens in chow-fed mice were associated with reduced type-2 immune function, we speculated that chow diets may enhance type-1 or type-3/17 responses due to the reciprocal regulation of T-helper cell subsets (29) and, thus, promote resistance to a pathogen where these responses are important. Contrary to our expectations, mice infected with the bacterial pathogen *C. rodentium*, where immunity is dependent on type-3-driven induction of interleukin (IL)-22 and expression of anti-microbial peptides such as Reg3γ, also had significantly higher pathogen burdens when fed with chow compared to SSD (Fig. 2A). This effect was also associated with increased levels of *C. rodentium*-specific IgG2a in serum (Fig. 2B). We next measured the expression of *Il22* and *Nos2* (encoding the inducible nitric oxide synthase) in the colon, as both genes are known to be strongly induced by *C. rodentium* infection (30, 31). However, we observed that expression was equivalent between dietary treatments (Fig. 2C and D). Thus, SSD consumption was associated with reduced susceptibility to two different enteric pathogens.

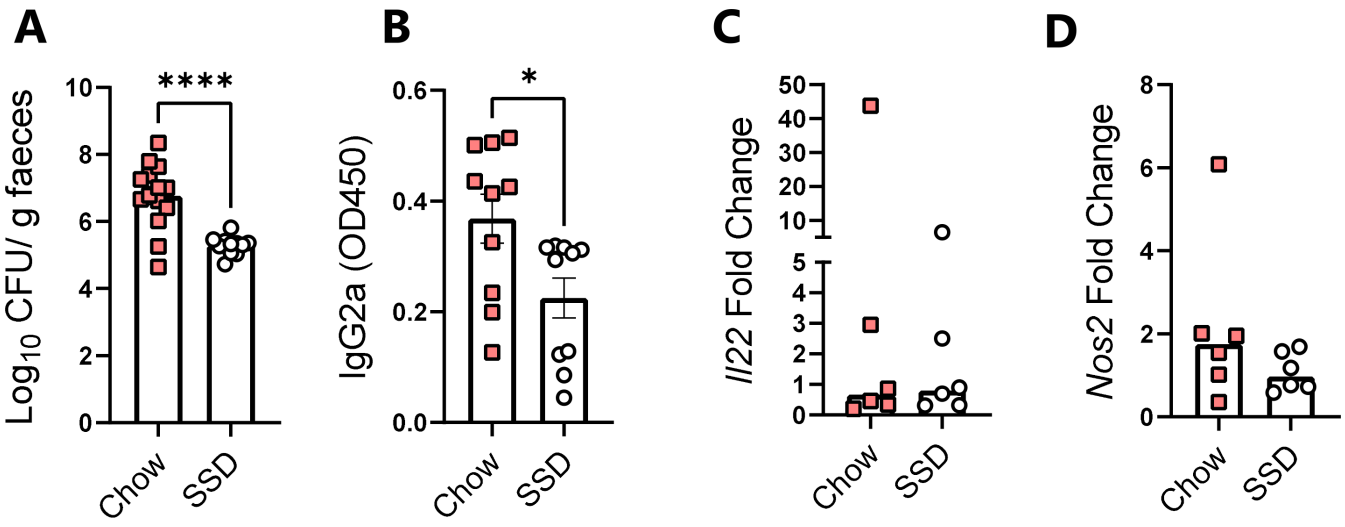

FIG 2 Impact of chow or SSDs on *C. rodentium* infection burdens and host immune response. Mice were fed with either chow or SSDs, infected with *C. rodentium*, and sacrificed 8 days p.i. (A) Fecal *C. rodentium* burdens on Day 8 p.i. $^{****}P < 0.001$ by unpaired *t*-test. (B) *C. rodentium*-specific IgG2a levels in serum on Day 8 p.i. $^{*}P < 0.05$ by unpaired *t*-test. (C and D) Expression of *Il22* and *Nos2* in colon on Day 8 p.i. Fold changes are relative to the infected chow-fed mice. Data are from three independent experiments, each with $n = 3$–6 mice/dietary group (A), two independent experiments, each with $n = 6$ mice/group (B), or a single experiment with $n = 6$/dietary group (C and D), and presented as mean ± S.E.M. (A and B) or medians (C and D).

Enriching SSDs with inulin increases pathogen burdens

Chow is a complex mixture of different components with a high level of crude, soluble fibers, in contrast to SSD that is devoid of soluble fiber and instead contains only insoluble cellulose. We therefore examined the effect of enriching SSD with inulin, a highly soluble fiber, on infection levels.

We have previously found that including inulin in SSD increased *T. muris* burdens in mice during acute infection (a single, high dose of 300 eggs), whereas cellulose fiber had no effect (32). To explore if trickle-infected mice also had higher *T. muris* burdens when fed with inulin, mice were fed with either SSD or inulin-enriched SSD and given the same trickle infection regime as above. Strikingly, we observed that mice fed with inulin-enriched SSD also had a substantially higher burden of *T. muris* than mice fed with SSD alone (Fig. 3A), with the effect being very similar to that of chow. Furthermore, in line with chow experiments, *C. rodentium*-infected mice fed with inulin-enriched SSD had higher infection burdens than those fed with SSD (Fig. 3B), which is consistent with a recent report (33). Thus, feeding with either unrefined chow, or SSD with an added source of purified soluble fiber, was sufficient to increase infection with two evolutionary divergent enteric pathogens.

Diet composition restructures the GM during *C. rodentium* and *T. muris* infection

To further explore the effect of the different diets on the gut environment, fecal samples taken from mice fed with chow, SSD, or inulin-enriched SSD with either *C. rodentium* or *T. muris* infection and their respective uninfected controls were analyzed for GM composition by 16S rRNA amplicon sequencing. Strong interactions were observed between diet

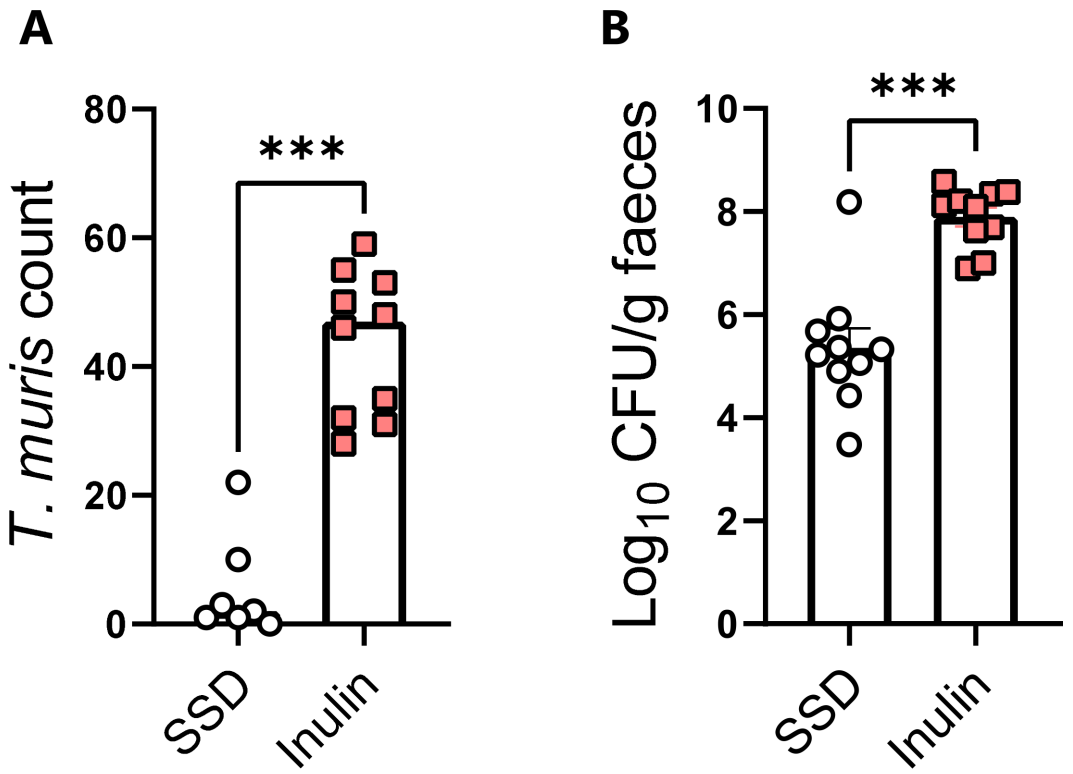

FIG 3 Impact of SSDs with or without inulin enrichment on *T. muris* and *C. rodentium* burdens. Mice were fed with either SSDs alone or SSD enriched with 10% inulin. Mice were trickle-infected with *T. muris* by inoculation with 20 eggs on Days 0, 7, and 14 and sacrificed on Day 35 or infected with *C. rodentium* and sacrificed on Day 8 p.i. (A) Caecal *T. muris* burdens on Day 35 p.i. Data are from two independent experiments with $n = 3–6$ mice/treatment group and shown as median values. ***$P < 0.001$ by Mann-Whitney test. (B) Fecal *C. rodentium* burdens at Day 8 p.i. ***$P < 0.001$ by unpaired *t*-test. Data are from two independent experiments, each with $n = 3–6$ mice/treatment group, and shown as mean ± S.E.M.

and infection. α-Diversity tended to be decreased by *C. rodentium* infection, at both observed species and Shannon index level (main effect of infection, $P = 0.07$ and $P = 0.052$, respectively; Fig. 4A). Diet had a substantially stronger effect with α-diversity metrics significantly higher in chow-fed mice than those fed with SSD, which likewise had a more diverse GM than inulin-fed mice ($P < 0.0001$ for main effect of diet; Fig. 4A). β-Diversity also differed significantly as a result of both diet and infection ($P < 0.05$ for interaction between diet and infection, permutational multivariate analysis of variance (PERMANOVA) on Bray-Curtis distance metrics; Fig. 4B). Pairwise testing revealed that infection tended (adjusted $P = 0.07$) to affect the GM only in chow-fed mice and not in SSD-fed or inulin-fed mice. Diet had a strong effect on the GM composition, which was largely independent of infection. In uninfected mice, the GM composition in SSD-fed animals was significantly different from those fed with either chow or inulin (adjusted $P < 0.05$), and chow and inulin also tended to result in distinct GM compositions (adjusted $P = 0.051$). Within infected mice, the same trend was evident but only significantly so for chow and SSD (adjusted $P < 0.05$). The main compositional changes resulting from

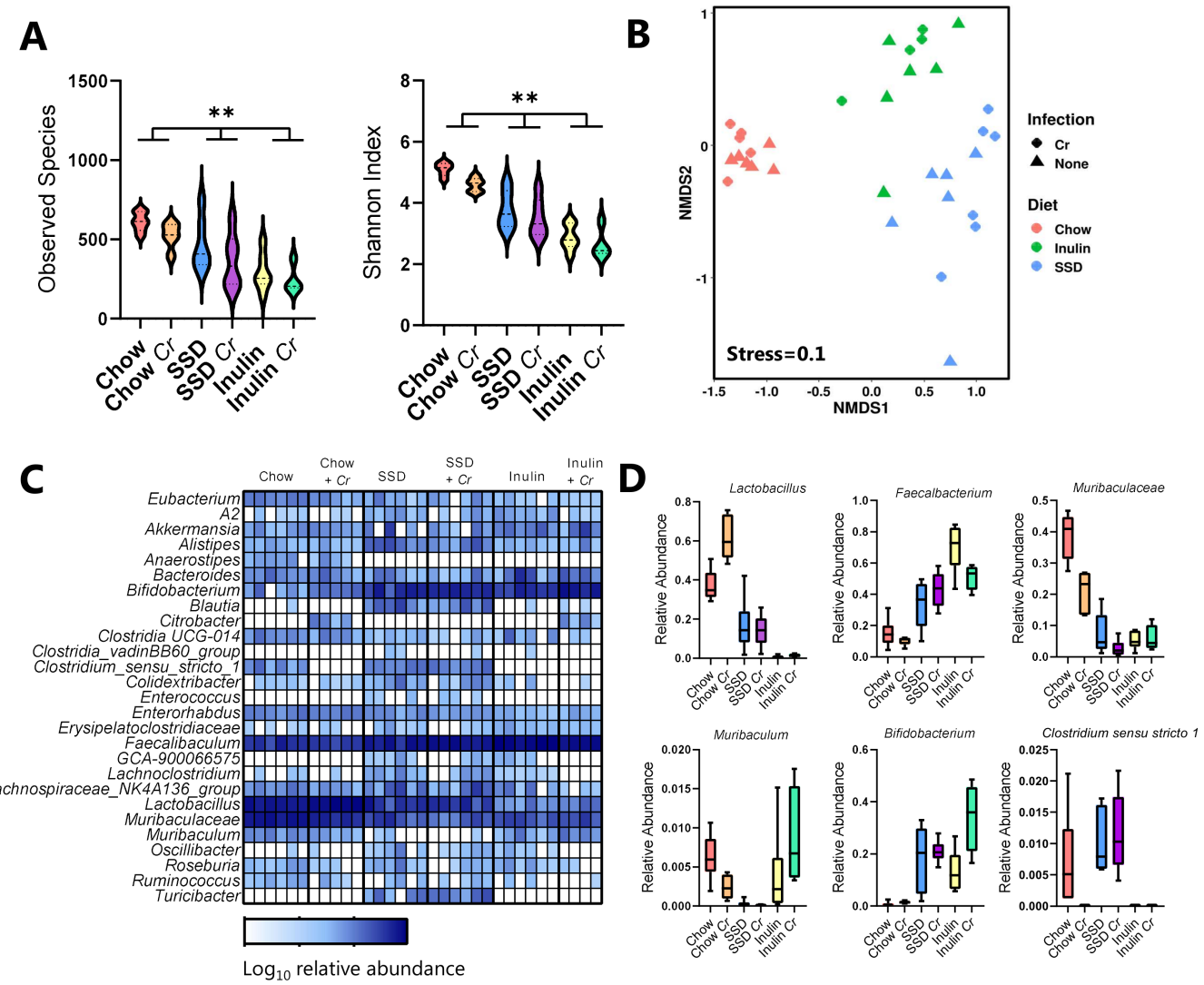

FIG 4 Impact of diet and *C. rodentium* infection on the host GM. Mice were fed with either chow, SSDs alone, or SSD enriched with 10% inulin. Mice were infected with *C. rodentium*, or left as uninfected controls, and fecal samples were collected at Day 7 p.i. $n = 4–6$/treatment group. (A) α-Diversity (observed species and Shannon index), in mice fed with chow, SSD, or inulin, with or without *C. rodentium* (*Cr*) infection. $^{**}P < 0.01$ illustrating main effect of diet by two-way ANOVA. (B) Non-metric multidimensional scaling (NMDS) plot showing β-diversity (based on Bray-Curtis dissimilarity metrics) of different treatment groups. (C) Relative abundance at genus or family (*Muribaculaceae*) level and (D) selected taxa in mice fed with chow, SSD, or inulin, with or without *Cr* infection.

the diet were a substantial reduction in the relative abundance of *Lactobacillus* spp. and the *Muribaculaceae* family in mice fed with SSD (with or without inulin enrichment) compared to chow and a corresponding increase in the *Faecalibacterium* and *Bifidobacterium* genera (Fig. 4C and D). Within the SSD diets, inulin enrichment resulted in an increase in the genera *Faecalibacterium* and *Muribaculum* and a reduction in *Clostridium sensu stricto 1*. These changes were further impacted by infection. For example, infection tended to increase *Lactobacillus* only in chow-fed mice and *Bifidobacterium* only in inulin-fed mice, while reductions in *Muribaculum* and *Clostridium sensu stricto 1* were apparent only in chow-fed mice (Fig. 4C and D). Overall, these data demonstrate that the different diets had a substantial effect on the underlying GM composition and that they influenced the response to *C. rodentium* infection, with only the GM of chow-fed and inulin-fed mice actively changing as a response to the pathogen.

A similar pattern was observed in the *T. muris* experiments. Diet had a strong influence on α-diversity, with uninfected chow-fed mice clearly having the most diverse GM. Infection significantly decreased this diversity in chow-fed mice; however, this effect was not evident in SSD- and inulin-fed mice ($P < 0.05$ for interaction between diet and infection; Fig. 5A). Diet and infection also exhibited strong interactions on β-diversity ($P < 0.05$ for interaction between diet and infection, PERMANOVA on Bray-Curtis distance metrics; Fig. 5B). Diet significantly impacted the GM composition, regardless of infection status (adjusted $P < 0.05$ for all PERMANOVA pairwise comparisons between diet groups in both uninfected and *T. muris*-infected mice). In contrast, the effect of infection was diet-dependent, with *T. muris* infection significantly impacting the GM only in chow-fed and inulin-fed mice (adjusted $P < 0.05$ for PERMANOVA pairwise comparisons) but not in SSD-fed mice (Fig. 5B). In the absence of infection, chow diets favored the growth of *Lactobacillus* spp. and the *Muribaculaceae* family, while SSD (with and without inulin) promoted the growth of *Faecalibacterium*, consistent with the *C. rodentium* study. Notably, *T. muris* infection also promoted *Lactobacillus* abundance that was most pronounced in inulin-fed mice, as well as the relative abundance of *Bifidobacterium* (Fig. 5C and D). However, the relative abundance of the genera *Enterococcus* and *Escherichia/Shiga* was also increased by *T. muris* infection, most drastically in the inulin-fed mice (Fig. 5C and D). Furthermore, we noted that infection also significantly decreased the abundance of *Alistipes* spp., most prominently in chow-fed and inulin-fed mice. Thus, consistent with the effects of diet on worm burden, the chow and inulin diet most strongly enabled *T. muris*-induced dysbiosis, while the effect of infection on the SSD diet was far more subtle.

Dietary inulin increases *T. muris* and *C. rodentium* burdens through distinct mechanisms

Given that the addition of inulin to SSD was sufficient to increase both *T. muris* and *C. rodentium* burdens, we next sought to determine whether this resulted from a common mechanism. Inulin-mediated susceptibility to acute, high-dose *T. muris* infection can be reversed by neutralization of IFNγ, thus manipulating the type-1/type-2 immune balance in favor of type-2 immunity (32). In contrast, it has recently been reported that higher burdens of *C. rodentium* in mice fed with inulin-enriched SSD appear to be independent of the immune response, as similar effects were observed in mice deficient in IL-18, IL-22, or adaptive immune cells ($Rag1^{-/-}$) (33). This suggests that the increased burdens of *T. muris* and *C. rodentium* may reflect two distinct mechanisms. To examine this issue in more detail, we harvested caecal or colon tissue from *T. muris*- or *C. rodentium*-infected mice, respectively, after feeding them with either SSD or inulin-enriched SSD. Transcriptomic profiling of caecum tissue from *T. muris*-infected mice revealed a dramatic remodeling of the host immune response. More than 1,900 genes were significantly regulated (adjusted $P < 0.05$, fold change > 2; File S1), with many of the upregulated genes being involved in pro-inflammatory or type-1-related immune responses (Fig. 6A). These included genes such as *Ifng*, *Il27*, and *Cxcl10*, which have all been implicated in inhibiting resistance to *T. muris* (34–36). In contrast, type-2-related genes such as *IL4*, *IL13*,

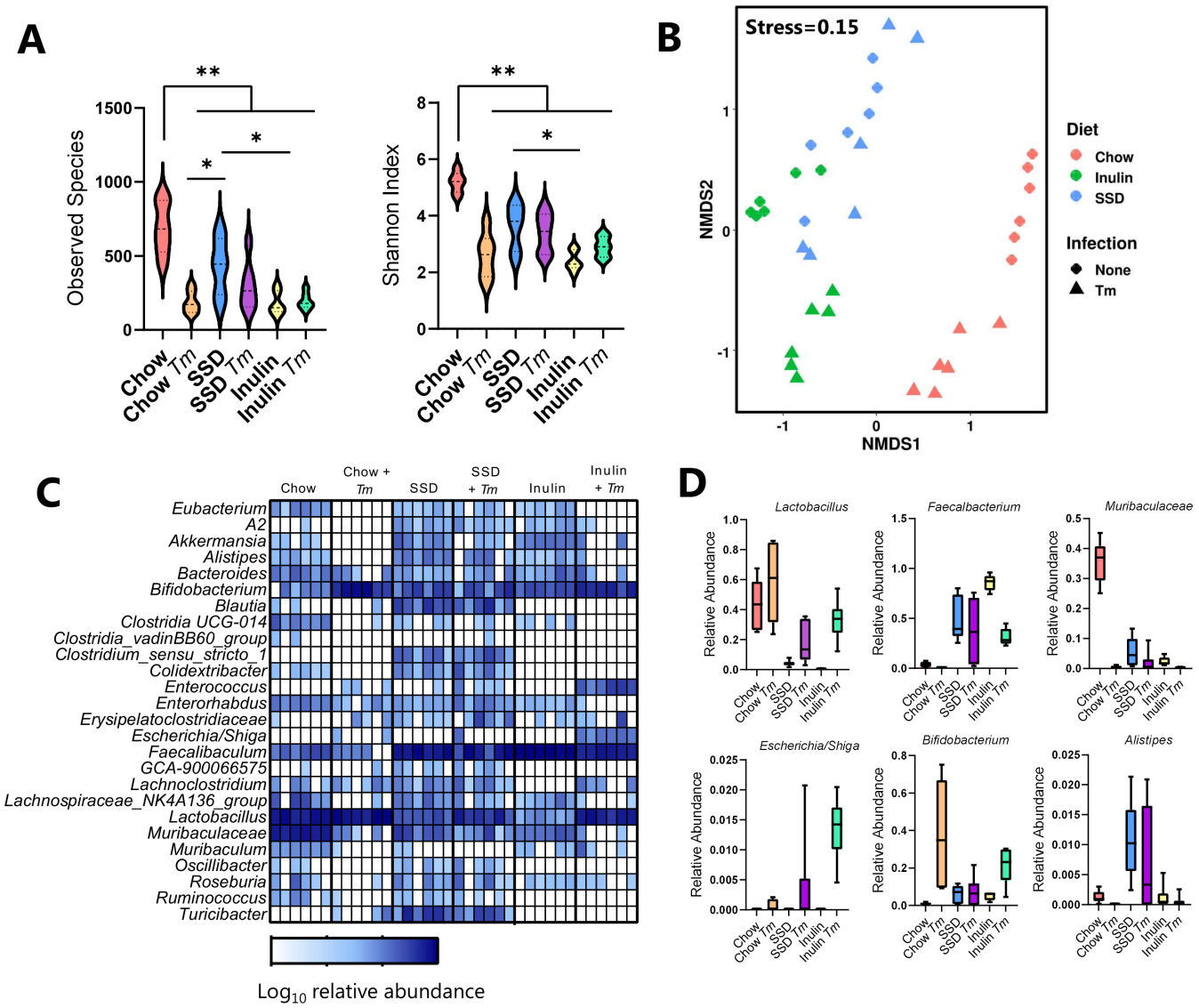

FIG 5 Impact of diet and *T. muris* infection on the host GM. Mice were fed with either chow, SSDs alone, or SSD enriched with 10% inulin. Mice were infected with *T. muris*, or left as uninfected controls, and fecal samples were collected at Day 35 following the commencement of trickle infection (20 eggs were given at Days 0, 7, and 14 p.i.). *n* = 6/treatment group. (A) α-Diversity (observed species and Shannon index), in mice fed with chow, SSD, or inulin, with or without *T. muris* (*Tm*) infection. $^{**}P < 0.01$, and $^{*}P < 0.05$ by two-way ANOVA, with Tukey's post hoc testing where interaction term is significant. (B) Non-metric multidimensional scaling (NMDS) plot showing β-diversity (based on Bray-Curtis dissimilarity metrics) of different treatment groups. (C) Relative abundance at genus or family (*Muribaculaceae*) level and (D) selected taxa in mice fed with chow, SSD, or inulin, with or without *Tm* infection.

and *Ang4*, all of which have been shown to be important for *T. muris* expulsion (36, 37), were suppressed (Fig. 6A). Among the top 10 upregulated genes in inulin-fed mice were *Nos2* and *Gzmk*, encoding a granzyme normally found in cytotoxic T cells and involved in antibacterial immune responses (Fig. 6B). Downregulated genes included *Mxpt1*, encoding a mucosal pentraxin, as well as genes encoding other mucosal defense molecules such as intelectins that are important for anti-helminth immunity (Fig. 6B). Finally, gene-set enrichment analysis (GSEA) revealed that the upregulated gene pathways were related not only to cell cycle processes (e.g., DNA replication) but also to cytokine signaling, anti-viral (RIG-I-like receptor signaling) responses, and anti-bacterial (Toll-like receptor and NOD-like receptor signaling) responses (Fig. 6C). Downregulated pathways were associated with diverse physiological roles such as calcium signaling and neuroactive ligand-receptor interactions (Fig. 6C). Taken together, these data suggest

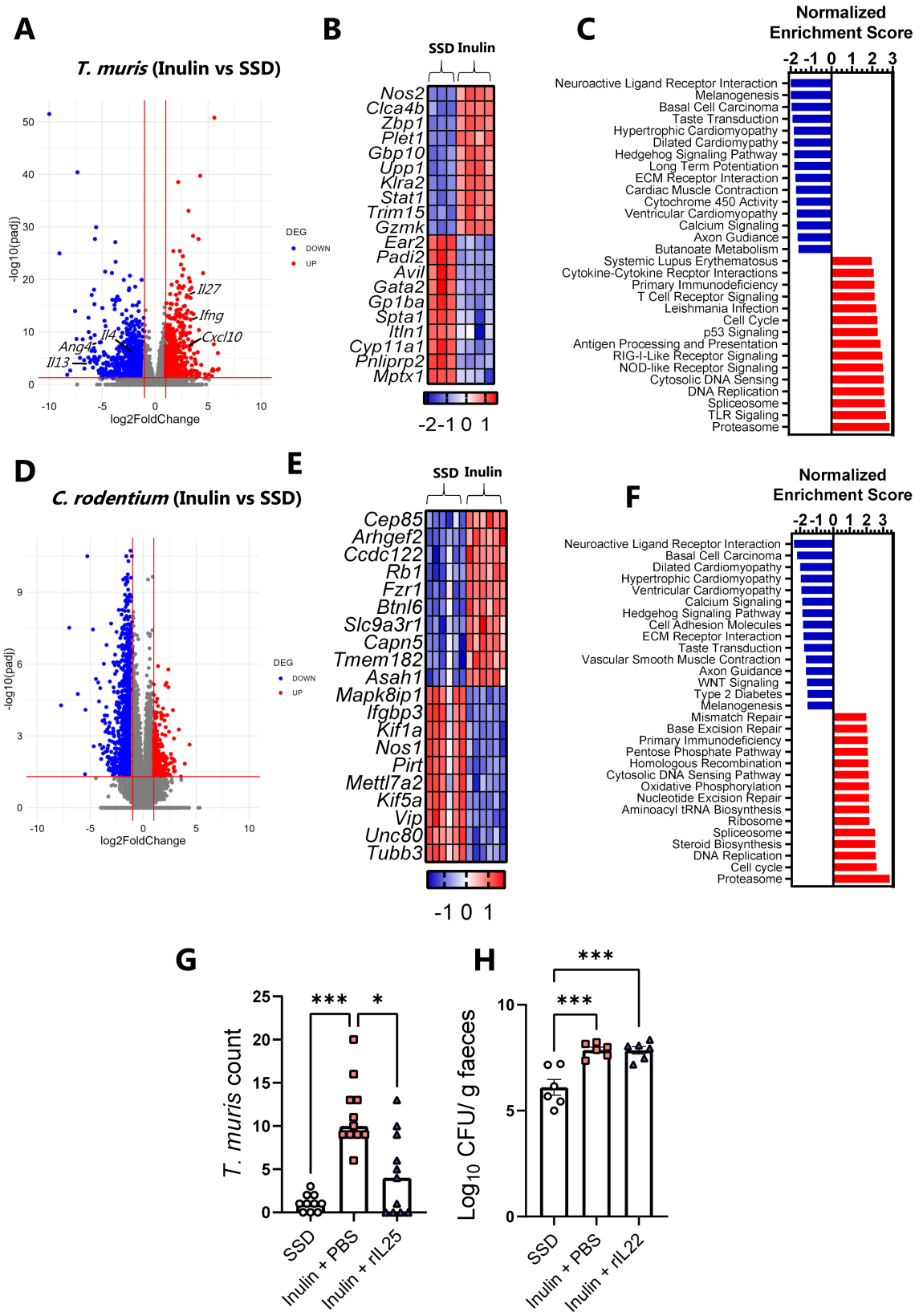

FIG 6 Transcriptomic analysis and cytokine administration reveal independent mechanisms for increased *T. muris* and *C. rodentium* burdens by dietary inulin. (A–F) Mice were fed either SSDs alone or SSD enriched with 10% inulin. Mice were trickle-infected with *T. muris* by inoculation with 20 eggs on Days 0, 7, and 14, and were sacrificed on Day 35 (n = 3–4/dietary group) (A–C) or infected with *C. rodentium* and sacrificed on Day 8 p.i. (n = 6/dietary group (**D–F**). (A and

(Continued on next page)

FIG 6 (Continued)

D) Volcano plots showing differentially expressed genes (adjusted $P < 0.05$; fold change > 2). (B and E) Heat map showing *Z*-scores of top 10 upegulated and downregulated genes as assessed by adjusted *P* values. A full list of significantly regulated genes is shown in File S1. (C and F) Top 15 Kyoto Encyclopedia of Genes and Genomes (KEGG) pathways enriched or suppressed by feeding inulin relative to SSD ($q < 0.05$), identified by GSEA. (G) Worm burdens in caecum on Day 21 p.i. following infection with 20 *T. muris* eggs in mice fed with SSD, inulin + vehicle control (PBS), or inulin + rIL-25. Data are from two independent experiments, each with $n = 5–6$ mice/treatment group, and are shown as median values. ***$P < 0.005$, and *$P < 0.05$ by Kruskal-Wallis test followed by Dunn's post hoc testing. (H) Fecal *C. rodentium* burdens on Day 8 p.i. in mice fed with SSD, inulin + vehicle control (PBS), or inulin + rIL-22. $n = 6$ mice/treatment group from a single experiment. Data are shown as mean ± S.E.M. ***$P < 0.005$ by Tukey's post hoc testing following one-way ANOVA.

that inulin promotes an inappropriate type-1-biased immune response during a low-dose trickle infection, which results in parasite chronicity and associated inflammation.

Next, the colonic transcriptomic response to dietary inulin in *C. rodentium*-infected mice was investigated. Relative to mice fed with SSD alone, mice fed with inulin-enriched SSD had altered expression of approximately 2,000 genes (Fig. 6D; File S1). However, unlike *T. muris*, few of these genes were involved in immune function. Inspection of the top 10 upregulated and downregulated genes showed that most were associated with metabolic and cell cycle processes such as centrosome function (*Cep85*), Rho GTPases (*Arhgef2*), tubulin activity (*Tubb3*), and neuropeptide signaling (*Vip*) (Fig. 6E). Similar to experiments with *T. muris*-infected mice, downregulated pathways identified by GSEA included calcium signaling and neuroactive ligand-receptor interactions. A number of pathways related to cardiac myopathy were also inhibited by inulin in both infection models, as a consequence of the suppression of many genes encoding voltage-dependent calcium channels (e.g., *Cacng4*) and cAMP formation (e.g., *Adcy3*). Enriched gene pathways included proteasome and spliceosome function (both also observed in *T. muris*-infected mice) and pathways related to ribosome activity and nucleotide excision and repair (Fig. 6F). A closer inspection of genes known to be involved in immunity to *C. rodentium* (38, 39) revealed no significant suppression related to inulin intake (File S1). For instance, *Il22* and *Reg3g* expression was not affected by inulin, while expression of *Il18* was significantly enhanced (fold change of +1.5), and *Il27* also tended to be enhanced (fold change of +2.6; adjusted *P* value of 0.13). Genes encoding β-defensins were either unchanged or, in the case of *Defb45*, significantly enhanced in inulin-fed mice (File S1). Overall, these results indicate that while inulin-mediated enhancement of *T. muris* infection was associated with impaired immune function, enhancement of *C. rodentium* infection was manifested despite a seemingly intact immune response, suggesting that the mechanisms through which diet increases pathogen burdens are different.

To test this in more detail, we reasoned that strengthening the type-2 response in *T. muris*-infected mice fed with inulin should restore resistance to infection, whereas equivalent support of the immune response in inulin-fed *C. rodentium*-infected mice would not have the same effect as an appropriate immune response was already generated. To this end, we fed mice with inulin-enriched SSD and gave them a single dose of 20 *T. muris* eggs. Mice were then treated with exogenous IL-25, a cytokine that stimulates a broad type-2 immune response in mucosal tissues (40) or vehicle control. Compared to mice fed with SSD alone, inulin again resulted in a drastic increase in worm burden, whereas mice treated with IL-25 had significantly less worms than inulin-fed mice given vehicle control (Fig. 6G). Thus, administration of a type-2 polarizing factor was sufficient to lower infection during inulin consumption. In contrast, the administration of IL-22 was not able to lower the burdens of *C. rodentium* in inulin-fed mice. Mice fed with inulin had higher fecal burdens of *C. rodentium* than mice fed with SSD (Fig. 6H), and these burdens were equivalent in IL-22-treated or vehicle control mice. Thus, these data support the notion that dietary inulin impairs type-2 immunity toward *T. muris* infection but enhances *C. rodentium* burdens by a mechanism independent of immune function.

Feeding chow or inulin-enriched SSDs has less pronounced effects on the course of small intestinal pathogen infections

Given that *T. muris* and *C. rodentium* share a relative similar tissue niche in the LI, we were also interested to see if these dietary effects were applicable to pathogens residing in the more proximal part of the gut, that is, the duodenum and jejunum. We selected the helminth *Heligmosomoides polygyrus* and the protozoa *Giardia muris* as two

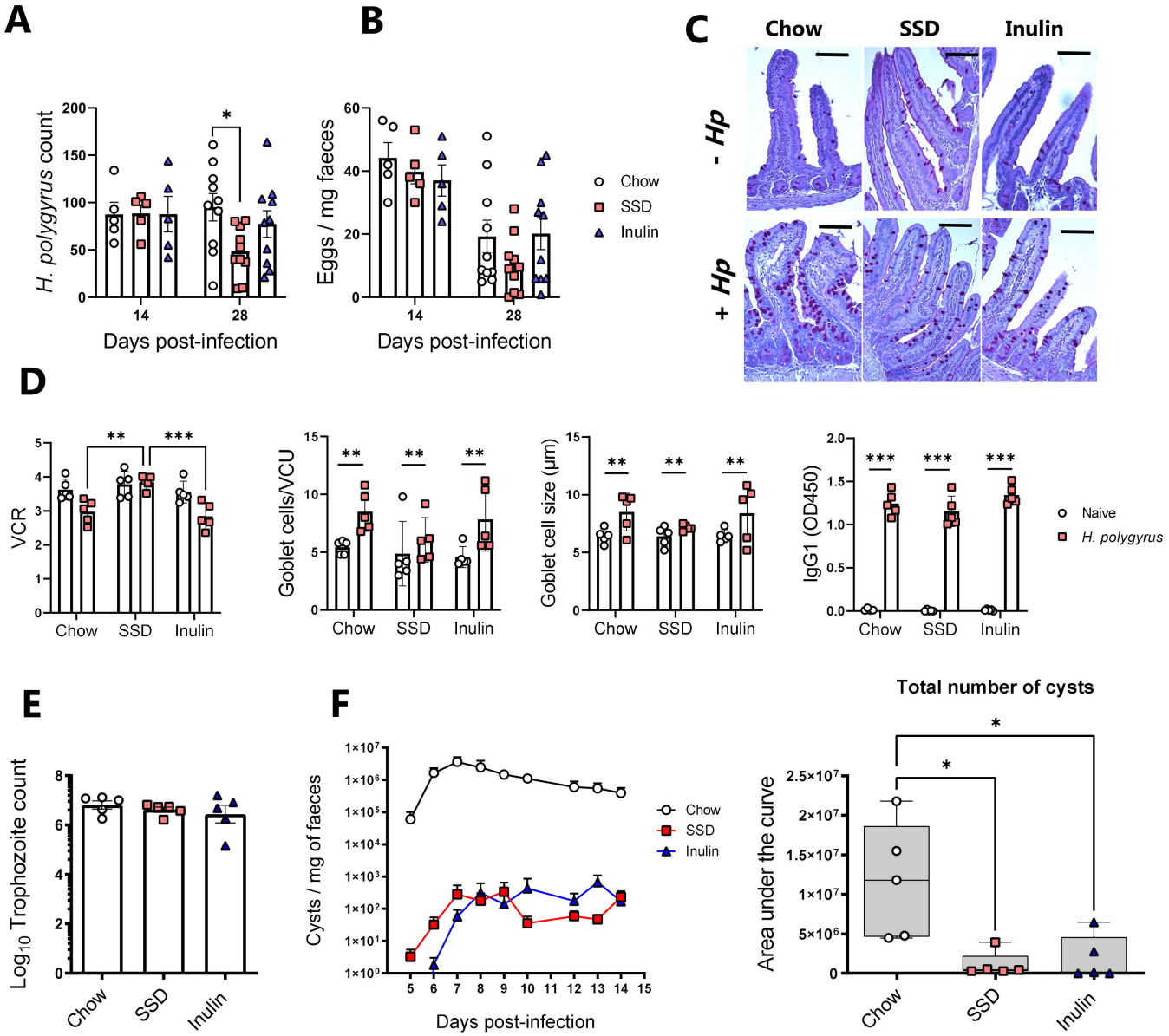

FIG 7 Impact of chow or SSDs with or without inulin enrichment on *Heligmosomoides polygyrus* and *Giardia muris* burdens. Mice were fed with either chow, SSDs alone, or SSD enriched with 10% inulin. Mice were infected with *H. polygyrus* and sacrificed on either Day 14 or Day 28 p.i. or with *G. muris* and sacrificed on Day 16 p.i. Data are shown as mean ± S.E.M. (A) *H. polygyrus* worm burdens in SI and (B) fecal egg counts on Days 14 and 28 p.i. **P* < 0.05 by Tukey's post hoc testing following one-way ANOVA at each time point. Data are from two independent experiments, each with *n* = 5/treatment group (Day 28 p.i.), or from a single experiment with *n* = 5 (Day 14 p.i.). (C and D) Assessment of VCR, goblet cell numbers and goblet cell diameter in the proximal jejunum, and *H. polygyrus*-specific IgG1 levels in serum, of mice at Day 28 p.i. with or without *H. polygyrus* infection and fed with different diets. Data are from a single experiment with *n* = 5/treatment group. ****P* < 0.005, and ***P* < 0.01 by two-way ANOVA, with Tukey's post hoc testing where interaction term is significant. Scale bar = 50 µm. ×200 magnification. (E) *G. muris* trophozoite counts in the SI on Day 16 p.i. (F) Daily *G. muris* cyst output in feces and cumulative cyst counts (total cyst number) over the course of infection from Day 5 until Day 14 p.i. **P* < 0.05 by Kruskal-Wallis test and Dunn's post hoc testing. Data are from a single experiment with *n* = 5/treatment group.

taxonomically distinct pathogens to assess this possibility. We observed that *H. polygyrus* burdens were similar between dietary groups at Day 14 p.i., but at Day 28 p.i., SSD-fed mice had lower worm burdens than chow-fed mice (but not inulin-fed mice; Fig. 7A). Fecal egg counts were also lower in SSD-fed mice at Day 28 p.i. but not significantly (Fig. 7B). Assessment of jejunum histology samples at Day 28 p.i. showed that villous height to crypt depth ratios (VCRs) were suppressed by *H. polygyrus* infection in chow-fed and inulin-fed mice but not SSD-fed mice ($P < 0.05$ for interaction between diet and infection; Fig. 7C and D). However, goblet cell numbers and size were increased by *H. polygyrus* comparably in all groups ($P < 0.05$ for main effect of infection, Fig. 7C and D). Moreover, serum IgG1 levels were equivalent in infected mice fed with different diets ($P < 0.05$ for main effect of infection Fig. 7D). None of these parameters were affected by diet in the absence of infection (Fig. 7D). *G. muris* trophozoite counts were equivalent in the SI of mice fed with either chow, SSD, or inulin-enriched SSD (Fig. 7E). Interestingly, cyst output was significantly lower in mice fed with SSD (with or without inulin), compared to chow (Fig. 7F). Thus, while diet composition also had effects on *H. polygyrus* infection and may influence the transmissibility of small intestinal protozoa, the effects on infection intensity were noticeably lower than with the caecum- and colon-dwelling pathogens. While we cannot rule out that these differential effects are intrinsic to the different pathogens studied and not their location in the gut, it does raise the possibility that tissue niche has an influence on the regulation of enteric pathogens by dietary factors.

Diet composition regulates the gut microbiota composition and primes mucosal tissue differentially in the colon and SI

To further explore whether the different tissue sites (SI vs. LI) may respond differently to the change in diet composition, we first assessed the mucosal tissue architecture following 14 days of diet adaption (i.e., the point of pathogen infection). In both the jejunum and colon, goblet cell numbers were not affected by the different diets, and VCRs in the jejunum were equivalent between dietary groups (Fig. 8A). However, we noted that crypt lengths in the colon tended to be shorter in mice fed with SSD than those fed with chow or inulin ($P = 0.07$; Fig. 8A). Given that we also observed the same phenomenon following extended consumption of SSD during *T. muris* experiments (Fig. 1), we speculated that the colon may be a more responsive site to the changes in diet composition. The LI represents the main site of microbial fermentation in the gut, and, therefore, it may be plausible that increased microbial loads in different tissue sites may differentially affect how these tissues respond to pathogen infection. Therefore, we assessed GM composition in both the SI and LI (caecum and proximal colon) in mice fed with chow, SSD, or inulin, for 14 days. α-Diversity was lower in mice fed with SSD compared to chow and was also substantially lower in the SI than in the colon, suggesting a richer GM composition in the LI (Fig. 8B). Moreover, total bacterial load as assessed by 16S quantitative PCR (qPCR) was also significantly higher in the LI than the SI ($P < 0.0001$) and also tended to be lower in SSD-fed mice than those fed with chow or inulin ($P = 0.09$ for effect of diet; Fig. 8C). Analysis of β-diversity again showed a significant interaction between diet and infection (Fig. 8D; $P < 0.01$ by PERMANOVA on Bray-Curtis distance metrics); however, pairwise testing did not identify significant difference between groups following multiple comparison adjustment. Notably, the taxonomical composition of the LI closely reflected that observed after longer periods of diet consumption observed previously (Fig. 4 and 5), suggesting rapid adaption of the GM to the tested diets (Fig. S3). The dominant taxa in both the LI and SI were *Faecalibaculum*, *Bifidobacterium*, *Lactobacillus,* and the *Muribaculaceae* family, with the LI additionally harboring a number of genera such as *Bacteroides*, *Blautia*, *Alistipes*, and *Roseburia* that were mostly absent in the SI (Fig. S3). Thus, while the exact mechanisms that lead to the altered pathogen loads remain to be revealed, our data show that the degree of diet-mediated susceptibility to infection correlates with the total bacterial load at the infection site.

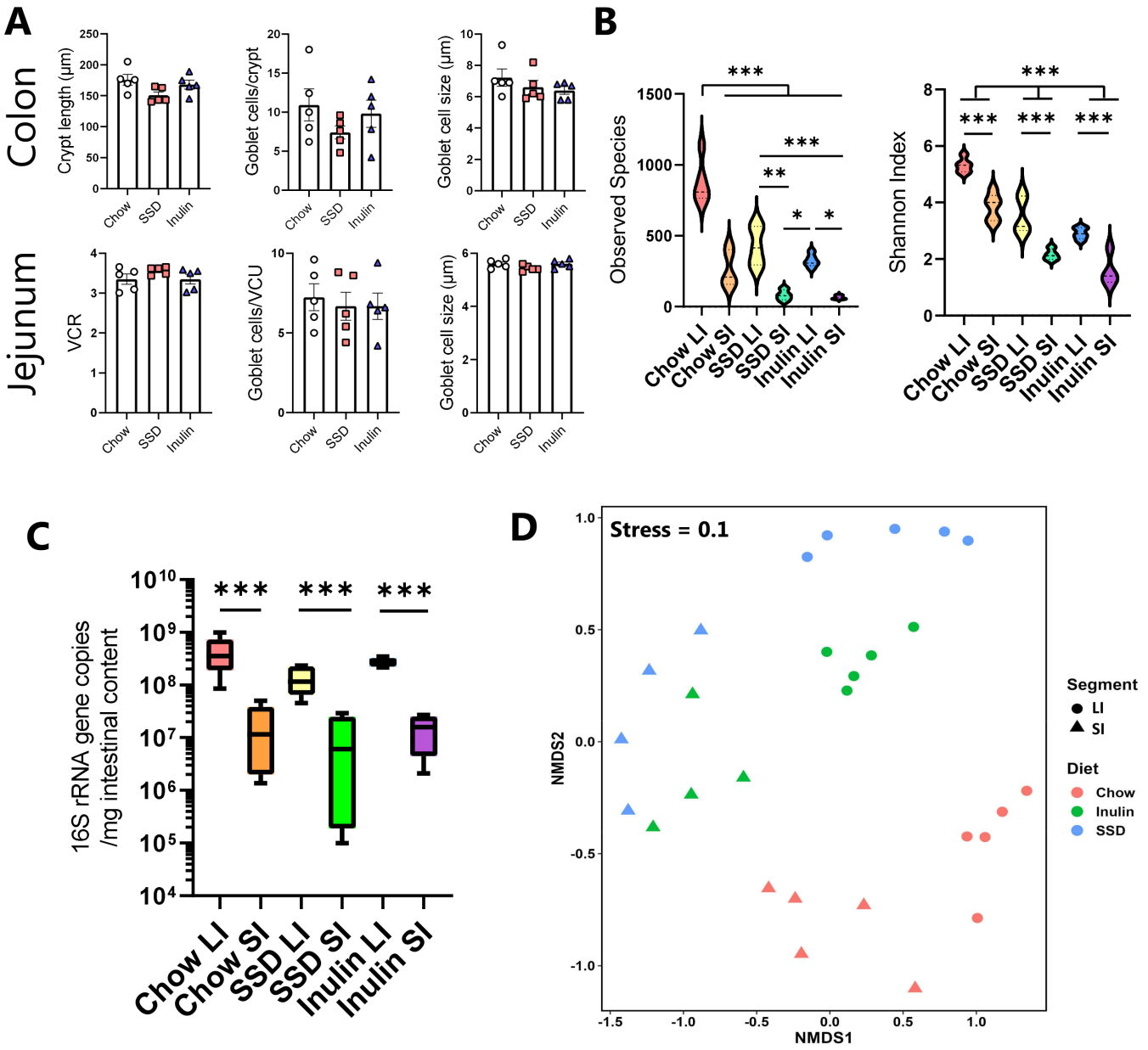

FIG 8 Impact of different diets on mucosal histology and microbiome composition in the SI and colon prior to infection. Mice were fed with either chow, SSDs alone, or SSD enriched with 10% inulin for 14 days. *n* = 4–5/group. (A) Colonic crypt lengths, jejunum VCR, and goblet cell numbers and size in the jejunum and colon. *n* = 5/group. Data shown are means ± S.E.M. (B) α-Diversity (observed species and Shannon index), in the LI and SI in mice fed with chow, SSD, or inulin. ***$P < 0.005$, **$P < 0.01$, and *$P < 0.05$ by two-way ANOVA, with Tukey's post hoc testing where interaction term is significant. (C) Total bacterial load in LI and SI in mice fed with different diets, assessed by qPCR of 16S rRNA gene copy number. ***$P < 0.005$, by two-way ANOVA. (D) Non-metric multidimensional scaling (NMDS) plot showing β-diversity (based on Bray-Curtis dissimilarity metrics) of different treatment groups.

DISCUSSION

In the current work, we present data that show that diet composition is a key factor in determining the severity of enteric infections in the caecum and colon of mice. Our results build on a growing body of literature that suggests that intestinal infections may be highly sensitive to the levels of different dietary components.

The consumption of whole-grain foods and soluble fibers is generally considered to promote gut health by reducing inflammation and stimulating the growth of beneficial, metabolite-producing microbes, such as short-chain fatty acid (SCFA)-producing gut

bacteria (11). SCFAs such as butyrate have been shown to have many beneficial effects, including providing a fuel source for oxidation in colonic epithelial cells and suppressing the growth of pathogenic bacteria (41, 42). However, while this paradigm holds true in many pre-clinical models of chronic diseases, there is evidence that, in some contexts, putatively healthy dietary components may negatively impact the gut environment. For example, the inclusion of refined inulin powder in SSD can exacerbate colitis and even lead to hepatic cancer in mice (43, 44), and we have found that the acute expulsion of a high dose of *T. muris* in C57BL/6 mice is impaired in mice fed with inulin-enriched SSD (32). We have now extended this to show that while feeding rodent with chow allows the establishment of a chronic *T. muris* trickle infection, as has previously been reported (28), feeding with SSD results in substantially lower worm burdens and appears to promote stronger type-2 anti-helminth immunity. These results thus challenge the paradigm that whole-grain-containing diets with large amounts of unrefined plant material are protective against enteric pathogens. Interestingly, we also showed that this effect is also applicable to *C. rodentium*. Of note, several recent reports have demonstrated similar findings. An et al. (33) also showed that colonization with *C. rodentium* was enhanced in mice fed with either chow or inulin-enriched SSD, relative to SSD, while Smith et al. (45) have found that large amounts of resistant starch incorporated into SSD also promote higher *C. rodentium* burdens. Similarly, *Salmonella* burdens also appeared to be enhanced by chow in comparison to SSD (27).

The precise mechanisms whereby diet composition drives this enhanced susceptibility to infection remain yet unresolved, although our current data suggest that the mechanisms are different between *T. muris* and *C. rodentium*. An et al. (33) proposed that feeding SSD to mice, which is low in fermentable fiber, results in a loss of commensal gut microbes and a nutrient-poor gut environment that does not support *C. rodentium* colonization. In contrast, the inclusion of fermentable fibers allows the production of microbial-derived metabolites, such as the SCFAs acetate and propionate. These metabolites, particularly acetate, can be directly utilized as energy sources by *C. rodentium* (33), providing a mechanistic basis for the increased *C. rodentium* colonization. However, An et al. (33) also showed that while the initial establishment of *C. rodentium* is higher in mice fed with chow in long-term experiments, these mice are capable of clearing the infection 2–3 weeks after colonization, whereas mice fed with SSD retained a low-level chronic infection. This suggests that the presence of a rich and diverse microbiome allows early colonization with pathogenic bacteria but that the commensal microbes eventually outcompete and exclude the pathogen. In contrast, a nutrient-deprived gut environment shaped by SSD will result in lower initial establishment, but those bacteria that do establish will persist over a longer period as there is less competition from commensals. This is in line with our experiments that show that increased *C. rodentium* establishment in inulin-fed mice is not accompanied by obvious defects in immunity as revealed by RNA-sequencing analysis and is not reversed by treatment with IL-22, a known stimulator of anti-*Citrobacter* immunity (39). Interestingly, most of the top upregulated genes (e.g., *Cep85*) in inulin-fed mice infected with *C. rodentium* were related to basic cellular processes such as centromere function and other cell cycle activities. The reasons for this can only be speculated on, but one possibility is that the enhanced bacterial levels in these mice stimulate increased cellular turnover and repair mechanisms that necessitate the need for upregulation of pathways related to cell cycle processes. This proposed mechanism is clearly different to how chow and inulin enhance *T. muris* burdens. In this case, SSD results in rapid expulsion of the parasite while either chow or inulin consumption results in a long-term chronic infection, accompanied by a type-1-biased immune response that is known to be detrimental for helminth expulsion. In addition, we have previously shown that the increased numbers of *T. muris* worms in inulin-fed mice are not accompanied by increased SCFA production (32), suggesting that *T. muris* does not leverage inulin-induced SCFA production to promote its survival, in contrast to *C. rodentium*.

How diet composition drives this type-1 bias is an ongoing question. Immune cells in the gut are calibrated by continual exposure to both dietary compounds and GM-derived metabolites. The enrichment of these ligands through the consumption of more complex diets (as opposed to highly simple and refined SSD) may result in the tuning of host intestinal immune processes toward a type-1 response and away from the protective type-2 response. Evidence for switches in the type-1/type-2 axis in response to dietary cues has been reported. For example, differences in the levels of dietary vitamin A or the activation of the aryl hydrocarbon receptor, a transcription factor highly sensitive to dietary compounds, can modulate innate lymphoid cell (ILC) balances to suppress ILC2 responses and render mice susceptible to helminths (46, 47). Of note, germ-free mice that are expected to have a very simple gut environment due to the absence of microbes to break down dietary fiber have exaggerated type-2 immune responses, suggesting a continuum between the complexity of the gut metabolic environment and the degree of polarization toward a type-1 response. However, it should be noted that inulin can influence host immune function even in the absence of a gut microbiota (48). Further experiments will be necessary to unravel these complex interactions between diet, infections, and the host immune system.

Our data also indicate that the enhancement of pathogen burdens by either chow or inulin-enriched SSD was more pronounced when infections were located in the LI rather than the SI. The reasons for this are not yet clear but may relate to the increased fermentative capacity of the caecum and colon relative to the SI, consequently exposing the pathogens to a more metabolically diverse environment. Interestingly, we observed that chow intake resulted in higher *G. muris* cyst output than SSD (regardless of inulin inclusion). The reasons for this, and why cyst output should be affected but not trophozoite numbers, are not clear and warrant further investigation. Potentially, a metabolic cue that stimulates the encysting of *G. muris* is suppressed when mice are fed with SSD. Overall, there appear to be conserved effects of diet across multiple, evolutionary distinct pathogens, but tissue niche may also be an important factor in diet-pathogen interactions. These conclusions are limited by the obvious fact that different pathogens are studied in the different gut compartments, and our data may simply reflect differences in pathogen life cycle and relationship with the host immune system, rather than an inherent effect of tissue predilection site.

In conclusion, we have shown that diet composition can affect enteric infection intensity in distinct murine infection models. The findings have clear relevance for the rational design of nutritional interventions with functional food components. Moreover, our results suggest that pharmacological or nutritional modulation of the gut environment may hold promise to develop novel therapeutic tools to limit infections and promote gut health.

MATERIALS AND METHODS

Mice and pathogens

C57BL/6 mice aged 6–7 weeks were used for all experiments and were sourced from either Envigo for *T. muris*, *C. rodentium*, or *H. polygyrus* experiments or Charles River for *G. muris* experiments. Mice were fed with either standard chow or, where indicated, purified open-source SSD [13 kJ% fat (E15051); ssniff Spezialdiäten GmbH, Germany] or SSD with 10% long-chain inulin replacing corn starch, as reported previously (32). Mice were fed for 2 weeks before infections commenced. *T. muris*, *H. polygyrus*, *C. rodentium*, and *G. muris* were propagated as described previously (30, 32, 49, 50). All infections were performed by oral gavage by dispensing a total volume of 0.2 mL/mouse. For *T. muris*, infections were performed by trickle-dosing with 20 eggs three times at 7-day intervals or, where mentioned, single doses of either 20 or 40 eggs. Infective doses for other pathogens were 10^9 *C. rodentium* CFU, 200 *H. polygyrus* third-stage larvae (L_3), or 10^4 *G. muris* cysts. All animal experimentation was approved by relevant committees (license number 2020-15-0201-00465 for *T. muris*, *H. polygyrus*, and *C. rodentium* infections and

EC2019/077 for *G. muris* experiments). Mice weights were monitored weekly, and welfare was assessed daily by experienced personnel. We observed no significant effects of diets or infection on weight gain. Mice were sacrificed at the indicated times p.i. *T. muris* and *H. polygyrus* burdens were determined with a dissecting microscope. Worm egg counts were assessed using a modified McMaster technique. *C. rodentium* loads in fecal samples were determined by serial dilution and plating overnight at 37°C on MacConkey agar. *G. muris* trophozoites were counted using a hemocytometer after incubating the SI in phosphare buffered saline on ice, with shaking.

In vivo administration of cytokines

Where indicated, 5 µg of IL-25 (#587306; BioLegend), or sterile PBS as a vehicle control, was administered by intraperitoneal (i.p.) injection every other day between Days 3 and 11 following *T. muris* infection, and 5 µg of IL-22 (#576206; BioLegend), or PBS, was administered by i.p. injection on Days 0, 2, and 4 following *C. rodentium* infection.

MLN collection and flow cytometry

MLNs were dissected, passed through a 70-µm cell strainer, and suspended in PBS supplemented with 2% fetal calf serum. Cells were washed and surface-stained with fluorescein isothiocyanate-conjugated hamster anti-mouse TCRb (clone H57-597; BD Biosciences) and PerCP-Cy5.5-conjugated rat anti-CD4 (clone RM4-5; BD Biosciences), followed by intracellular staining with Alexa Fluor 647-conjugated mouse anti-mouse T-bet (clone 4B10; BD Biosciences), PE-conjugated rat anti-mouse GATA3 (clone TWAJ; Thermo Fisher Scientific), or FITC-conjugated rat anti-mouse Foxp3 (FJK-16s; Thermo Fisher Scientific). Cells were analyzed on a BD Accuri C6 Flow Cytometer (BD Biosciences), and data were analyzed using Accuri CFlow Plus Software (Accuri Cytometers). Gating strategy is shown in Fig. S4.

Histology

Colon or jejunum samples were fixed in 4% paraformaldehyde, before paraffin wax embedding, sectioning, and periodic acid-Schiff staining. Goblet cells were determined in five colonic crypts or five jejunum villous-crypt units per mouse. Goblet cell diameters were measured for 10 randomly selected cells per mouse. Tissue sections were photographed using a Leica DFC480 camera, and measurements were performed using LAS v4.6 software (Leica, Switzerland).

RNA extraction and qPCR

RNA was extracted from full-thickness caecum or colon tissues as previously described (30). cDNA was synthesized using Quantitect Reverse Transcription Kits (Qiagen), and qPCR was carried out using the following program: 95°C for 2 min followed by 40 cycles of 15 s at 95°C and 20 s at 60°C. *Gapdh* was used as a reference gene for normalization, and fold changes were calculated using the ΔΔCT method. Primer sequences are listed in Table 1.

RNA sequencing

RNA was used for 150-bp paired-end Illumina NovaSeq6000 sequencing (Novogene, Cambridge, UK). Raw sequences were mapped to the mm10 genome assembly and read counts generated, which were used to determine differentially expressed genes using DEseq2 (51). Pathway analysis was conducted using GSEA (52). Volcano plots were constructed using R package ggplot2 (3.4.3) (53).

16S rRNA amplicon sequencing

Fresh feces were collected after defecation from mice in the *T. muris* and *C. rodentium* studies. Alternatively, intestinal content from the SI (full length) or LI (caecum and

TABLE 1 Primer sequences used for qPCR

Gene	Forward primer (5′–3′)	Reverse primer (5′–3′)
Gapdh	TATGTCGTGGAGTCTACTGGT	GAGTTGTCATATTTCTCGTGG
Ifng	GACTGTGATTGCGGGGTTGTA	TCACTGCAGCTCTGAATGTTTCT
Il13	GGCAGCATGGTATGGAGTGT	CTTGCGGTTACAGAGGCCAT
Il22	CGCTGCCCGTCAACACCCGG	CTGATCTTTAGCACTGACTCCTCG
Nos2	GGTGAAGGGACTGAGCTGTT	TGCACTTCTGCTCCAAATCCA

proximal colon) was collected after 14 days of diet adaption. Samples were immediately placed on ice before transfer to –80°C within 1 h of collection. DNA was extracted using a FastDNA Spin Kit for soil (MP Biomedicals, USA), including bead beating. 16S RNA amplicons (Regions 1–8, bV18-A) were prepared using the following primers: 8F, AGRGTTYGATYMTGGCTCAG; and 1391R, GACGGGCGGTGWGTRCA. The PCR program was initial denaturation at 98°C for 3 min, 25 cycles of amplification (98°C for 30 s, 62°C for 20 s, and 72°C for 2 min), and a final elongation at 72°C for 5 min. Sequencing libraries were prepared from purified amplicons using the SQKLSK114 Kit (Oxford Nanopore Technologies, UK) according to the manufacturer's protocol with the following modifications: 500-ng total DNA was used as input, and CleanNGS SPRI beads (CleanNA, the Netherlands) were used for library cleanup steps. Libraries were loaded onto a MinION R10.4.1 flowcell and sequenced using MinKNOW 22.12.7 software (Oxford Nanopore Technologies, UK).

Analysis of 16S rRNA amplicon data

The sequencing reads in the demultiplexed and basecalled fastq files were filtered for length (320- to 2,000-bp fragments selected) and quality (phred score of >15) using a local implementation of Filtlong (github.com//rrwick/Filtlong) v0.2.1 with the settings –min_length 320 – max_length 2000 –min_mean_q 97. The SILVA 16S/18S rRNA 138 SSURef NR99 full-length database in RESCRIPt format was downloaded from QIIME (54, 55). Potential generic placeholders and dead-end taxonomic entries were cleared from the taxonomy flat file; that is, entries containing uncultured, metagenome, or unassigned were replaced with a blank entry. The filtered reads were mapped to the SILVA 138.1 99% NR database with minimap2 v2.24r-1122 using the -ax map-ont command (56) and downstream processing using SAMtools v1.14 (57). Mapping results were filtered such that query sequence length relative to alignment length deviated <5%. Noteworthy, low-abundantOperational taxonomic units making up <0.01% of the total mapped reads within each sample were disregarded as a data denoising step. Further bioinformatic processing was done via RStudio IDE (2022.2.3.492) running R version 4.2.3 (20230315) and using the following R packages: ampvis2 (2.7.27) (58), tidyverse (1.3.1), seqinR (4.2.16), ShortRead (1.54.0), and iNEXT (2.0.20) (59, 60). Analysis of β-diversity was carried out using non-parametric microbial interdependence test and PERMANOVA (999 permutations) on Bray-Curtis dissimilarly metrics, followed by pairwise testing with Adonis using R package vegan (2.6.4) (61), applying Bonferroni corrections for adjusted *P* values.

qPCR for total bacterial load

The total bacterial load was quantified using universal 16S rRNA probe and primers (F, TCCTACGGGAGGCAGCAGT; and R, GGACTACCAGGGTATCTAATCCTGTT) as previously described (62), utilizing a linearized plasmid containing the PCR amplicon from *E. coli* as standard.

Enzyme-linked immunosorbent assay

Excretory/secretory antigens from *T. muris* and *H. polygyrus* were produced as previously described (32). *C. rodentium* antigens were produced by homogenization of cultured

bacterial pellet in lysis buffer (CellLytic B, Sigma-Aldrich) followed by centrifugation and harvesting of the soluble protein antigens. Serum IgG1 and IgG2a specific for the different antigens were determined by enzyme-linked immunosorbent assay as previously described (63).

Statistical analysis

P values of <0.05 were considered significant. Assumptions of normality were checked through Shapiro-Wilk tests or inspection of histogram plots and Kolmogorov-Smirnov tests of ANOVA residuals. Parametric data were analyzed using unpaired *t*-tests, or two-way ANOVA and Tukey's post hoc testing, and presented as means ± S.E.M. Non-parametric data were $\log_{10}$-transformed prior to two-way ANOVA, with the results presented as geometric means and 95% confidence intervals. Alternatively, non-parametric data were analyzed using Mann-Whitney tests or Kruskal-Wallis and Dunn's post hoc tests, and results were presented as median values. Details of each experiment are given in the appropriate figure legends.

ACKNOWLEDGMENTS

We are grateful to Pankaj Arora, Mette Schjelde, Penile Jensen, Stig Thamsborg, Emil Jakobsen, and Joshua Malsa for their assistance. This work was supported by Independent Research Fund Denmark (grants 7026-0094B and 2034-00245B), the Novo Nordisk Foundation (grants 0052422 and NNF22OC0074714), and the A.P. Møller Foundation (grant 20-L-0300).

AUTHOR AFFILIATIONS

[1]Department of Veterinary and Animal Sciences, Faculty of Health and Medical Sciences, University of Copenhagen, Frederiksberg, Denmark
[2]Department of Translational Physiology, Infectiology and Public Health, Faculty of Veterinary Medicine, Laboratory of Parasitology, Ghent University, Merelbeke, Belgium

AUTHOR ORCIDs

John E. Olsen http://orcid.org/0000-0001-6225-6587
Andrew R. Williams http://orcid.org/0000-0002-8231-282X

FUNDING

Funder	Grant(s)	Author(s)
Novo Nordisk Fonden (NNF)	0052422	Andrew R. Williams
Danmarks Frie Forskningsfond (DFF)	7026-0094B	Andrew R. Williams
A.P. Møller Fonden | Fonden til Lægevidenskabens Fremme (A.P. Møller Fonden til Lægevidenskabens Fremme)	Grant 20-L-0300	Andrew R. Williams

AUTHOR CONTRIBUTIONS

Helene Israelson, Conceptualization, Formal analysis, Investigation, Writing – review and editing | Amalie Vedsted-Jakobsen, Investigation, Writing – review and editing | Ling Zhu, Investigation, Writing – review and editing | Aurelie Gagnaire, Formal analysis, Investigation, Writing – review and editing | Alexandra von Münchow, Investigation, Writing – review and editing | Nina Polakovicova, Investigation, Methodology, Writing – review and editing | Angela H. Valente, Investigation, Methodology, Writing – review and editing | Ali Raza, Investigation, Writing – review and editing | Audrey I. S. Andersen-Civil, Investigation, Methodology, Writing – review and editing | John E. Olsen, Methodology, Resources, Writing – review and editing | Laura J. Myhill, Investigation, Methodology, Writing – review and editing | Peter Geldhof, Conceptualization, Methodology,

Resources, Supervision, Writing – review and editing | Andrew R. Williams, Conceptualization, Formal analysis, Funding acquisition, Investigation, Methodology, Supervision, Writing – original draft, Writing – review and editing

DATA AVAILABILITY

Raw RNA-sequence data are available at GEO under accession number GSE223377. 16S rRNA amplicon sequence data are available at SRA under BioProject Accession number PRJNA1016163.

ADDITIONAL FILES

The following material is available online.

Supplemental Material

File S1 (mBio02603-23-S0001.xlsx). Differentially expressed genes from RNAseq.
Supplemental Material (mBio02603-23-S0002.pdf). Figures S1-S4.

REFERENCES

1. Anonymous. 2017. Estimates of global, regional, and national morbidity, mortality, and aetiologies of diarrhoeal diseases: a systematic analysis for the global burden of disease study 2015. Lancet Infect Dis 17:909–948.
2. Loukas A, Maizels RM, Hotez PJ. 2021. The yin and yang of human soil-transmitted helminth infections. Int J Parasitol 51:1243–1253. https://doi.org/10.1016/j.ijpara.2021.11.001
3. Boeriu A, Roman A, Fofiu C, Dobru D. 2022. The current knowledge on *Clostridioides difficile* infection in patients with inflammatory bowel diseases. Pathogens 11:819. https://doi.org/10.3390/pathogens11070819
4. Charlier J, Thamsborg SM, Bartley DJ, Skuce PJ, Kenyon F, Geurden T, Hoste H, Williams AR, Sotiraki S, Höglund J, Chartier C, Geldhof P, van Dijk J, Rinaldi L, Morgan ER, von Samson-Himmelstjerna G, Vercruysse J, Claerebout E. 2018. Mind the gaps in research on the control of gastrointestinal nematodes of farmed ruminants and pigs. Transbound Emerg Dis 65 Suppl 1:217–234. https://doi.org/10.1111/tbed.12707
5. Charlier J, Barkema HW, Becher P, De Benedictis P, Hansson I, Hennig-Pauka I, La Ragione R, Larsen LE, Madoroba E, Maes D, Marín CM, Mutinelli F, Nisbet AJ, Podgórska K, Vercruysse J, Vitale F, Williams DJL, Zadoks RN. 2022. Disease control tools to secure animal and public health in a densely populated world. Lancet Planet Health 6:e812–e824. https://doi.org/10.1016/S2542-5196(22)00147-4
6. Sheikh BA, Bhat BA, Mir MA. 2022. Antimicrobial resistance: new insights and therapeutic implications. Appl Microbiol Biotechnol 106:6427–6440. https://doi.org/10.1007/s00253-022-12175-8
7. González-Quilen C, Rodríguez-Gallego E, Beltrán-Debón R, Pinent M, Ardévol A, Blay MT, Terra X. 2020. Health-promoting properties of proanthocyanidins for intestinal dysfunction. Nutrients 12:130. https://doi.org/10.3390/nu12010130
8. Morrison KE, Jašarević E, Howard CD, Bale TL. 2020. It's the fiber, not the fat: significant effects of dietary challenge on the gut microbiome. Microbiome 8:15. https://doi.org/10.1186/s40168-020-0791-6
9. vanAMA, Wetzels SMW, Wouters K, Vanmierlo T, van deJ, deC, Schalkwijk CG. 2021. Dietary advanced glycation endproducts (ages) increase their concentration in plasma and tissues, result in inflammation and modulate gut microbial composition in mice; evidence for reversibility. Food Research International 147:110547.
10. Anhê FF, Varin TV, Le Barz M, Desjardins Y, Levy E, Roy D, Marette A. 2015. Gut microbiota dysbiosis in obesity-linked metabolic diseases and prebiotic potential of polyphenol-rich extracts. Curr Obes Rep 4:389–400. https://doi.org/10.1007/s13679-015-0172-9
11. Blander JM, Longman RS, Iliev ID, Sonnenberg GF, Artis D. 2017. Regulation of inflammation by microbiota interactions with the host. Nat Immunol 18:851–860. https://doi.org/10.1038/ni.3780
12. Valle-Noguera A, Ochoa-Ramos A, Gomez-Sánchez MJ, Cruz-Adalia A. 2021. Type 3 innate lymphoid cells as regulators of the host-pathogen interaction. Front Immunol 12:748851. https://doi.org/10.3389/fimmu.2021.748851
13. El-Naccache DW, Haskó G, Gause WC. 2021. Early events triggering the initiation of a type 2 immune response. Trends Immunol 42:151–164. https://doi.org/10.1016/j.it.2020.11.006
14. Buck MD, Sowell RT, Kaech SM, Pearce EL. 2017. Metabolic instruction of immunity. Cell 169:570–586. https://doi.org/10.1016/j.cell.2017.04.004
15. Barberi C, Campana S, De Pasquale C, Rabbani Khorasgani M, Ferlazzo G, Bonaccorsi I. 2015. T cell polarizing properties of probiotic bacteria. Immunol Lett 168:337–342. https://doi.org/10.1016/j.imlet.2015.11.005
16. Hang S, Paik D, Yao L, Kim E, Trinath J, Lu J, Ha S, Nelson BN, Kelly SP, Wu L, Zheng Y, Longman RS, Rastinejad F, Devlin AS, Krout MR, Fischbach MA, Littman DR, Huh JR. 2019. Bile acid metabolites control T(H)17 and T(reg) cell differentiation. Nature 576:143–148. https://doi.org/10.1038/s41586-019-1785-z
17. Vogt L, Ramasamy U, Meyer D, Pullens G, Venema K, Faas MM, Schols HA, de Vos P. 2013. Immune modulation by different types of β2→1-fructans is toll-like receptor dependent. PLoS One 8:e68367. https://doi.org/10.1371/journal.pone.0068367
18. Vogt LM, Elderman ME, Borghuis T, de Haan BJ, Faas MM, de Vos P. 2017. Chain length-dependent effects of inulin-type fructan dietary fiber on human systemic immune responses against hepatitis-B. Mol Nutr Food Res 61. https://doi.org/10.1002/mnfr.201700171
19. Williams AR, Klaver EJ, Laan LC, Ramsay A, Fryganas C, Difborg R, Kringel H, Reed JD, Mueller-Harvey I, Skov S, van Die I, Thamsborg SM. 2017. Co-operative suppression of inflammatory responses in human dendritic cells by plant proanthocyanidins and products from the parasitic nematode Trichuris suis. Immunology 150:312–328. https://doi.org/10.1111/imm.12687
20. Tu T, Koski KG, Scott ME. 2008. Mechanisms underlying reduced expulsion of a murine nematode infection during protein deficiency. Parasitology 135:81–93. https://doi.org/10.1017/S0031182007003617
21. Shi HN, Scott ME, Stevenson MM, Koski KG. 1994. Zinc deficiency impairs T cell function in mice with primary infection of *Heligmosomoides polygyrus* (Nematoda). Parasite Immunol 16:339–350. https://doi.org/10.1111/j.1365-3024.1994.tb00359.x
22. Zou J, Chassaing B, Singh V, Pellizzon M, Ricci M, Fythe MD, Kumar MV, Gewirtz AT. 2018. Fiber-mediated nourishment of gut microbiota protects against diet-induced obesity by restoring IL-22-mediated colonic health. Cell Host Microbe 23:41–53. https://doi.org/10.1016/j.chom.2017.11.003
23. Chambers ES, Byrne CS, Morrison DJ, Murphy KG, Preston T, Tedford C, Garcia-Perez I, Fountana S, Serrano-Contreras JI, Holmes E, Reynolds CJ, Roberts JF, Boyton RJ, Altmann DM, McDonald JAK, Marchesi JR, Akbar AN, Riddell NE, Wallis GA, Frost GS. 2019. Dietary supplementation with inulin-propionate ester or inulin improves insulin sensitivity in adults with overweight and obesity with distinct effects on the gut microbiota,

plasma metabolome and systemic inflammatory responses: a randomised cross-over trial. Gut 68:1430–1438. https://doi.org/10.1136/gutjnl-2019-318424
24. Wastyk HC, Fragiadakis GK, Perelman D, Dahan D, Merrill BD, Yu FB, Topf M, Gonzalez CG, Van Treuren W, Han S, Robinson JL, Elias JE, Sonnenburg ED, Gardner CD, Sonnenburg JL. 2021. Gut-microbiota-targeted diets modulate human immune status. Cell 184:4137–4153. https://doi.org/10.1016/j.cell.2021.06.019
25. Anhê FF, Nachbar RT, Varin TV, Trottier J, Dudonné S, Le Barz M, Feutry P, Pilon G, Barbier O, Desjardins Y, Roy D, Marette A. 2019. Treatment with camu camu (*Myrciaria dubia*) prevents obesity by altering the gut microbiota and increasing energy expenditure in diet-induced obese mice. Gut 68:453–464. https://doi.org/10.1136/gutjnl-2017-315565
26. Neumann M, Steimle A, Grant ET, Wolter M, Parrish A, Willieme S, Brenner D, Martens EC, Desai MS. 2021. Deprivation of dietary fiber in specific-pathogen-free mice promotes susceptibility to the intestinal mucosal pathogen *Citrobacter rodentium*. Gut Microbes 13:1966263. https://doi.org/10.1080/19490976.2021.1966263
27. Wolter M, Steimle A, Parrish A, Zimmer J, Desai MS, Rawls JF. 2021. Dietary modulation alters susceptibility to *Listeria monocytogenes* and *Salmonella* Typhimurium with or without a gut microbiota. mSystems 6:e0071721. https://doi.org/10.1128/mSystems.00717-21
28. Glover M, Colombo SAP, Thornton DJ, Grencis RK. 2019. Trickle infection and immunity to *Trichuris muris*. PLoS Pathog 15:e1007926. https://doi.org/10.1371/journal.ppat.1007926
29. Anthony RM, Rutitzky LI, Urban JF, Stadecker MJ, Gause WC. 2007. Protective immune mechanisms in helminth infection. Nat Rev Immunol 7:975–987. https://doi.org/10.1038/nri2199
30. Zhu L, Andersen-Civil AIS, Castro-Meija JL, Nielsen DS, Blanchard A, Olsen JE, Thamsborg SM, Williams AR. 2022. Garlic-derived metabolites exert antioxidant activity, modulate gut microbiota composition and limit *Citrobacter rodentium* infection in mice. Antioxidants (Basel) 11:2033. https://doi.org/10.3390/antiox11102033
31. Smith AD, Botero S, Shea-Donohue T, Urban JF. 2011. The pathogenicity of an enteric *Citrobacter rodentium* infection is enhanced by deficiencies in the antioxidants selenium and vitamin E. Infect Immun 79:1471–1478. https://doi.org/10.1128/IAI.01017-10
32. Myhill LJ, Stolzenbach S, Mejer H, Jakobsen SR, Hansen TVA, Andersen D, Brix S, Hansen LH, Krych L, Nielsen DS, Nejsum P, Thamsborg SM, Williams AR. 2020. Fermentable dietary fiber promotes helminth infection and exacerbates host inflammatory responses. J Immunol 204:3042–3055. https://doi.org/10.4049/jimmunol.1901149
33. An J, Zhao X, Wang Y, Noriega J, Gewirtz AT, Zou J, Baumler AJ. 2021. Western-style diet impedes colonization and clearance of *Citrobacter rodentium*. PLoS Pathog 17:e1009497. https://doi.org/10.1371/journal.ppat.1009497
34. Sorobetea D, Svensson-Frej M, Grencis R. 2018. Immunity to gastrointestinal nematode infections. Mucosal Immunol 11:304–315. https://doi.org/10.1038/mi.2017.113
35. Artis D, Villarino A, Silverman M, He W, Thornton EM, Mu S, Summer S, Covey TM, Huang E, Yoshida H, Koretzky G, Goldschmidt M, Wu GD, de Sauvage F, Miller HRP, Saris CJM, Scott P, Hunter CA. 2004. The IL-27 receptor (WSX-1) is an inhibitor of innate and adaptive elements of type 2 immunity. J Immunol 173:5626–5634. https://doi.org/10.4049/jimmunol.173.9.5626
36. Cliffe LJ, Humphreys NE, Lane TE, Potten CS, Booth C, Grencis RK. 2005. Accelerated intestinal epithelial cell turnover: a new mechanism of parasite expulsion. Science 308:1463–1465. https://doi.org/10.1126/science.1108661
37. D'Elia R, DeSchoolmeester ML, Zeef LAH, Wright SH, Pemberton AD, Else KJ. 2009. Expulsion of *Trichuris muris* is associated with increased expression of angiogenin 4 in the gut and increased acidity of Mucins within the goblet cell. BMC Genomics 10:492. https://doi.org/10.1186/1471-2164-10-492
38. Muñoz M, Eidenschenk C, Ota N, Wong K, Lohmann U, Kühl AA, Wang X, Manzanillo P, Li Y, Rutz S, Zheng Y, Diehl L, Kayagaki N, van Lookeren-Campagne M, Liesenfeld O, Heimesaat M, Ouyang W. 2015. Interleukin-22 induces Interleukin-18 expression from epithelial cells during intestinal infection. Immunity 42:321–331. https://doi.org/10.1016/j.immuni.2015.01.011
39. Zheng Y, Valdez PA, Danilenko DM, Hu Y, Sa SM, Gong Q, Abbas AR, Modrusan Z, Ghilardi N, de Sauvage FJ, Ouyang W. 2008. Interleukin-22 mediates early host defense against attaching and effacing bacterial pathogens. Nat Med 14:282–289. https://doi.org/10.1038/nm1720
40. Owyang AM, Zaph C, Wilson EH, Guild KJ, McClanahan T, Miller HRP, Cua DJ, Goldschmidt M, Hunter CA, Kastelein RA, Artis D. 2006. Interleukin 25 regulates type 2 cytokine-dependent immunity and limits chronic inflammation in the gastrointestinal tract. J Exp Med 203:843–849. https://doi.org/10.1084/jem.20051496
41. Walker AC, Bhargava R, Vaziriyan-Sani AS, Pourciau C, Donahue ET, Dove AS, Gebhardt MJ, Ellward GL, Romeo T, Czyż DM. 2021. Colonization of the caenorhabditis elegans gut with human enteric bacterial pathogens leads to proteostasis disruption that is rescued by butyrate. PLoS Pathog 17:e1009510. https://doi.org/10.1371/journal.ppat.1009510
42. Salvi PS, Cowles RA. 2021. Butyrate and the intestinal epithelium: modulation of proliferation and inflammation in homeostasis and disease. Cells 10:1775. https://doi.org/10.3390/cells10071775
43. Singh V, Yeoh BS, Chassaing B, Xiao X, Saha P, Aguilera Olvera R, Lapek JD, Zhang L, Wang W-B, Hao S, Flythe MD, Gonzalez DJ, Cani PD, Conejo-Garcia JR, Xiong N, Kennett MJ, Joe B, Patterson AD, Gewirtz AT, Vijay-Kumar M. 2018. Dysregulated microbial fermentation of soluble fiber induces cholestatic liver cancer. Cell 175:679–694. https://doi.org/10.1016/j.cell.2018.09.004
44. Singh V, Yeoh BS, Walker RE, Xiao X, Saha P, Golonka RM, Cai J, Bretin ACA, Cheng X, Liu Q, Flythe MD, Chassaing B, Shearer GC, Patterson AD, Gewirtz AT, Vijay-Kumar M. 2019. Microbiota fermentation-NLRP3 axis shapes the impact of dietary fibres on intestinal inflammation. Gut 68:1801–1812. https://doi.org/10.1136/gutjnl-2018-316250
45. Smith A, Chen C, Cheung L, Ward R, Hintze K, Dawson H. 2022. Raw potato starch alters the microbiome, colon and cecal gene expression, and resistance to *Citrobacter rodentium* infection in mice fed a western diet. Current Developments in Nutrition 6:1028. https://doi.org/10.1093/cdn/nzac069.033
46. Li S, Bostick JW, Ye J, Qiu J, Zhang B, Urban JF, Avram D, Zhou L. 2018. Aryl hydrocarbon receptor signaling cell intrinsically inhibits intestinal group 2 innate lymphoid cell function. Immunity 49:915–928. https://doi.org/10.1016/j.immuni.2018.09.015
47. Spencer SP, Wilhelm C, Yang Q, Hall JA, Bouladoux N, Boyd A, Nutman TB, Urban JF, Wang J, Ramalingam TR, Bhandoola A, Wynn TA, Belkaid Y. 2014. Adaptation of innate lymphoid cells to a micronutrient deficiency promotes type 2 barrier immunity. Science 343:432–437. https://doi.org/10.1126/science.1247606
48. Fransen F, Sahasrabudhe NM, Elderman M, Bosveld M, El Aidy S, Hugenholtz F, Borghuis T, Kousemaker B, Winkel S, van der Gaast-de Jongh C, de Jonge MI, Boekschoten MV, Smidt H, Schols HA, de Vos P. 2017. β2→1-fructans modulate the immune system *in Vivo* in a microbiota-dependent and -independent fashion. Front Immunol 8:154. https://doi.org/10.3389/fimmu.2017.00154
49. Zhu L, Andersen-Civil AIS, Myhill LJ, Thamsborg SM, Kot W, Krych L, Nielsen DS, Blanchard A, Williams AR. 2022. The phytonutrient cinnamaldehyde limits intestinal inflammation and enteric parasite infection. J Nutr Biochem 100:108887. https://doi.org/10.1016/j.jnutbio.2021.108887
50. Maertens B, Gagnaire A, Paerewijck O, De Bosscher K, Geldhof P. 2021. Regulatory role of the intestinal microbiota in the immune response against *Giardia*. Sci Rep 11:10601. https://doi.org/10.1038/s41598-021-90261-z
51. Love MI, Huber W, Anders S. 2014. Moderated estimation of fold change and dispersion for RNA-seq data with DESeq2. Genome Biol 15:550. https://doi.org/10.1186/s13059-014-0550-8
52. Subramanian A, Tamayo P, Mootha VK, Mukherjee S, Ebert BL, Gillette MA, Paulovich A, Pomeroy SL, Golub TR, Lander ES, Mesirov JP. 2005. Gene set enrichment analysis: a knowledge-based approach for interpreting genome-wide expression profiles. Proc Natl Acad Sci U S A 102:15545–15550. https://doi.org/10.1073/pnas.0506580102
53. Wickham H. 2016. Ggplot2: elegant graphics for data analysis. Springer-Verlag, Cham.
54. Quast C, Pruesse E, Yilmaz P, Gerken J, Schweer T, Yarza P, Peplies J, Glöckner FO. 2013. The SILVA ribosomal RNA gene database project: liproved data processing and web-based tools. Nucleic Acids Res 41:D590–6. https://doi.org/10.1093/nar/gks1219

55. Yilmaz P, Parfrey LW, Yarza P, Gerken J, Pruesse E, Quast C, Schweer T, Peplies J, Ludwig W, Glöckner FO. 2014. The SILVA and "all-species living tree project (LTP). Nucl. Acids Res 42:D643–D648. https://doi.org/10.1093/nar/gkt1209
56. Li H. 2018. Minimap2: pairwise alignment for nucleotide sequences. Bioinformatics 34:3094–3100. https://doi.org/10.1093/bioinformatics/bty191
57. Danecek P, Bonfield JK, Liddle J, Marshall J, Ohan V, Pollard MO, Whitwham A, Keane T, McCarthy SA, Davies RM, Li H. 2021. Twelve years of SAMtools and BCFtools. Gigascience 10:giab008. https://doi.org/10.1093/gigascience/giab008
58. Albertsen M, Karst SM, Ziegler AS, Kirkegaard RH, Nielsen PH. 2015. Back to basics--the influence of DNA extraction and primer choice on phylogenetic analysis of activated sludge communities. PLoS One 10:e0132783. https://doi.org/10.1371/journal.pone.0132783
59. Hsieh TC, Ma KH, Chao A. 2016. iNEXT: an R package for rarefaction and extrapolation of species diversity. Hill numbers 7:1451–1456. https://doi.org/10.1111/2041-210X.12613
60. Chao A, Gotelli NJ, Hsieh TC, Sander EL, Ma KH, Colwell RK, Ellison AM. 2014. Rarefaction and extrapolation with hill numbers: a framework for sampling and estimation in species diversity studies. Ecological Monographs 84:45–67. https://doi.org/10.1890/13-0133.1
61. Oksanen J. 2010. Vegan: community cology package. Available from: http://veganr-forger-projectorg
62. Nadkarni MA, Martin FE, Jacques NA, Hunter N. 2002. Determination of bacterial load by real-time PCR using a broad-range (universal) probe and primers set. Microbiology (Reading) 148:257–266. https://doi.org/10.1099/00221287-148-1-257
63. Polakovicova N, Adji AV, Myhill LJ, Williams AR. 2023. Whipworm infection in mice increases coinfection of enteric pathogens but promotes clearance of *Ascaris* larvae from the lungs. J Infect Dis 227:1428–1432. https://doi.org/10.1093/infdis/jiad063